ACS OMEGA

http://pubs.acs.org/journal/acsodf

Article

Kinetic Model of Olefins/Isobutane Alkylation Using Sulfuric Acid as Catalyst

Zhicheng Xin, Hongbo Jiang,* Zhenyuan Zhang, Yushi Chen, and Jianping Wang

Cite This: *ACS Omega* 2022, 7, 9513−9526

Read Online

ACCESS | Metrics & More | Article Recommendations

ABSTRACT: The alkylation of isobutane and low molecular olefins using strong acid as catalysts is an important process in the petrochemical field, and its product, alkylate, is an ideal gasoline blending component due to high octane number, low vapor pressure, low sulfur, and lack of aromatics. To better meet the optimization process of the simulation of the alkylation unit, a reaction kinetic model with 20 reactions based on industrial data was developed, in which the alkylation products were divided into lumped components in detail. The reactor model was established based on the flow state and structural pattern of the industrial reactor, considering the internal circulation flow, and is suitable for the simulation of the DuPont alkylation process. Also, eventually, the model parameters were solved by the nonlinear least-squares fitting method. The results of the validation calculations showed that the kinetic model fitted the experimental data with good agreement. In addition, the reaction kinetic model was used to predict the influence of operating conditions, which is consistent with the trend in actual industrial production.

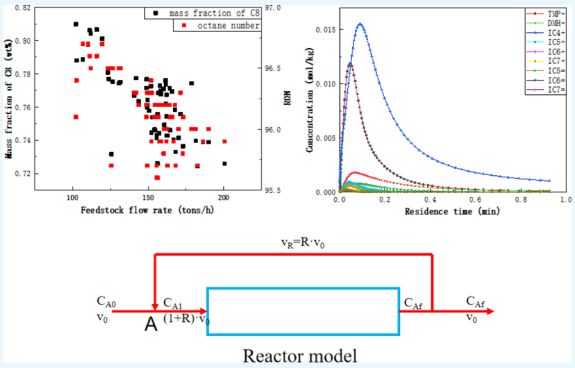

1. INTRODUCTION

In the oil refining industry, the alkylation process is an important process in which isobutane is used as the raw material and reacts with C_3−C_5 olefins using strong acid as catalyst to produce alkylates. The product has high octane number, low sulfur content, and no olefins or aromatics, which makes it a very ideal gasoline blending component.[1,2] The alkylate as a blending component of gasoline can not only increase its octane number but also dilute other gasoline components as a solvent and reduce the content of sulfur, olefins, and aromatics in gasoline.

With the continuous development of the automobile manufacturing industry, high-octane number gasoline with good antiknock performance has received more and more attention. In addition, the environmental regulations also have increasingly strict requirements for olefin, benzene, and aromatic content in gasoline. In China, the National VI standard[3] for gasoline released in 2016 has made significant downward adjustments to the upper limits of aromatic, olefin, and benzene content, which requires the aromatic content to be no more than 35%, benzene content to be no more than 0.8%, and olefin content to be no more than 18%, which indicates that high-octane number alkylates with the advantages of no aromatics, benzene, and olefins are becoming more and more popular.

Alkylation reactions need to be carried out in the presence of strong acid,[4,5] so the alkylation can be divided into three categories according to the physical properties of catalysts: liquid acid alkylation, solid acid alkylation, and ionic liquid acid alkylation. Liquid acids mainly include sulfuric acid and hydrofluoric acid, which are widely used in the alkylation process in the industry,[6] but there are many problems in safety and environmental protection. In response to the shortcomings of traditional liquid acids, solid acids and ionic liquid acids have received much attention in recent years because of their green and environmental advantages and have great potential to become the mainstream direction of alkylation catalyst development in the future. However, large-scale industrial production has not yet been realized because of the problems such as the easy deactivation of solid acid catalysts[7] and the expensive cost of ionic liquids.[8] Most of the alkylation processes currently used in the industry are processes using sulfuric acid as the catalyst because of the good economics of the sulfuric acid process and safer and more environmentally friendly operation than the hydrofluoric acid process.[9]

The alkylation reaction is a process controlled by both chemical reactions and diffusion, which is very complex and contains a series of reactions based on carbonium ions as intermediates.[10−12] It is generally believed that the mass transfer

Received: December 3, 2021
Accepted: February 23, 2022
Published: March 11, 2022

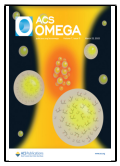

https://doi.org/10.1021/acsomega.1c06850
ACS Omega 2022, 7, 9513−9526

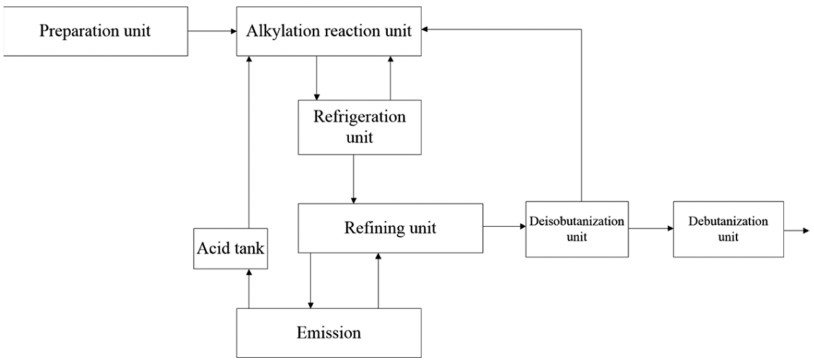

Figure 1. Brief procedure of the alkylation process.

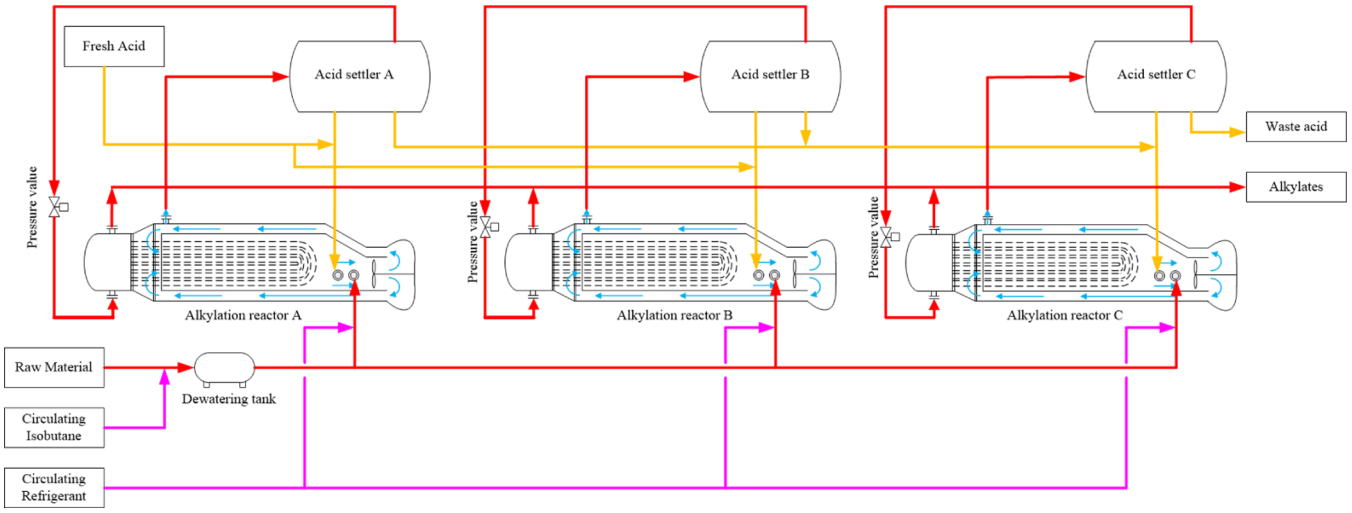

Figure 2. Alkylation reactor module.

from isobutane to the acid phase is the controlling step to determine the reaction rate. In the alkylation process, the mixing state of acid and hydrocarbon has a great influence on the selectivity and yield of the reaction because of the large difference in density and viscosity of the two phases. In addition, the reaction temperature, acid concentration, the volume ratio of acid to hydrocarbon, and the molar ratio of isobutane to olefins also have a significant effect on the yield.[13] The alkylation process must choose suitable conditions to operate efficiently. Daily analytical sampling alone is not only small in the amount of data obtained but also time-consuming. The study of kinetics, on the other hand, can not only provide information about the alkylation reaction under different conditions so as to effectively control the reaction and improve the efficiency of chemical production but also understand the kinetics of the side reactions, which can save raw materials and make the later products easy to separate, and it can also solve the kinetic equations to derive the optimal operating conditions of the device so that the device can operate efficiently under the best condition.

Many studies have been reported on the kinetics of alkylation. In the early 1940s, Schmerling[14,15] proposed a mechanism based on the carbonium ion principles to explain the alkylation process of olefins and isobutane. Subsequently, Albright et al.[16,17] explained the formation mechanism of acid−soluble hydrocarbons and red oil cations based on the abovementioned chain reaction principles. The author also pointed out that the isomerization of trimethylpentane (TMPs) carbonium ions was not the main source to produce dimethylhexane (DMH) carbonium ions because the amount of DMHs will change significantly with residence time and agitation conditions. Lee and Harriott[18] investigated the alkylation reaction and solved the kinetic model containing a main reaction and a polymerization reaction based on experimental data using the theory of mass transfer and chemical reaction simultaneously. Langley and Pike[19] established a 17-reaction mechanism model for the alkylation reaction kinetics of propylene and isobutane and treated the reaction rates of carbonium and olefin intermediates based on the assumption of steady-state rates to obtain the rate constants and activation energies of the model. Schilder et al.[20] studied the kinetics of the reaction of isobutane with 2-butene in a stirred tank reactor, focusing on the droplet size distribution of the IL catalyst BMIMCI/$AlCl_3$ dispersed in C_4 hydrocarbons. The intrinsic chemical rate constant was derived from the mean droplet size and the measured effective rate constant (including a possible influence of external or internal diffusion). According to the classical carbonium mechanism, Sun et al.[21] developed a kinetic model of alkylation reaction using sulfuric acid as catalyst and predicted the concentration changes in TMPs, DMHs, and heavy ends (HEs). The experimental and simulation data were in good agreement. However, most of the alkylation kinetics are based on laboratory research, and studies based on industrial data have not been carried out systematically.

In this paper, the reactor model was determined according to the structural pattern and flow state of the reactor. A kinetic model of alkylation reaction using sulfuric acid as catalyst was established to simulate the alkylation process, and its kinetic

https://doi.org/10.1021/acsomega.1c06850
ACS Omega 2022, 7, 9513−9526

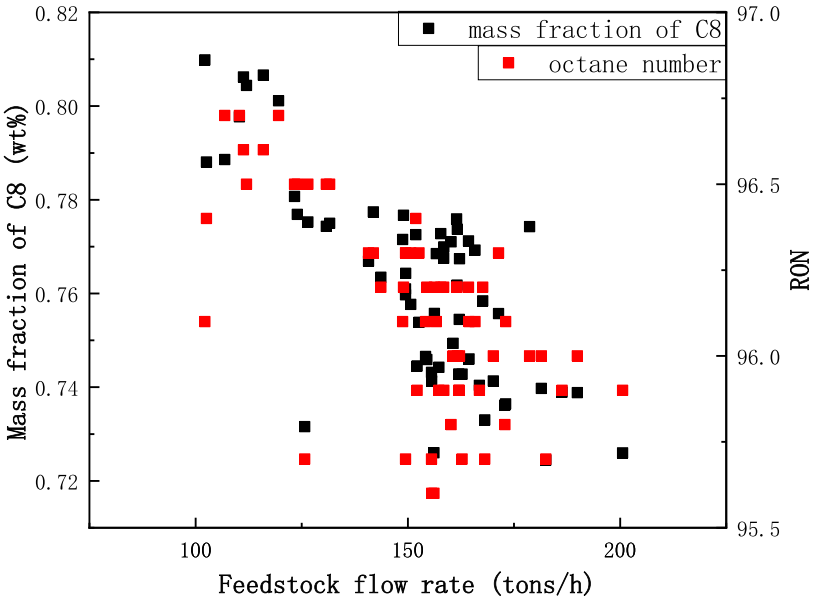

Figure 3. Influence of feed flow rate on the distribution of C_8 and RON.

parameters were estimated through industrial data regression. Industrial data and model calculation results are consistent with each other.

2. STUDY SUBJECT

2.1. Description of the Alkylation Process. The subject of the research is a sulfuric acid alkylation unit developed by Dupont[22,23] to produce high-octane gasoline blending components. Data were obtained from the industrial alkylation unit, including DCS data, monthly technical reports, material balances in a wide range of raw material composition, and flow rates. The principal scheme of the alkylation process implemented in the industry is presented in Figure 1.

After removing butadiene from the preparation unit, the raw material is mixed with the circulating isobutane stream recovered from the top of the de-isobutane tower and the circulating refrigerant stream obtained from the refrigeration cycle unit and then enters the alkylation reactors in three streams. At the same time, sulfuric acid from the acid settler and fresh acid are mixed into the alkylation reactor and mixed with the feed hydrocarbon in the reactor. Olefins and isobutane react under the catalysis of sulfuric acid to produce alkylates. After the reaction product and sulfuric acid flow out from the reactor, they flow through the acid settler, in which the hydrocarbon phase is separated from sulfuric acid. Then, sulfuric acid circulates back to the inlet of the reactor; the hydrocarbon phase from the acid settler passes through the pressure valve to lower the pressure to about 20 kPa where the light hydrocarbons are vaporized, thus absorbing the heat released from the alkylation reaction. The products from the tube side of the three reactors are mixed after heat exchange and then enter the downstream tank. Information about the flow of the alkylation reactor module is shown in Figure 2.

2.2. Industrial Conditions. In the data collected, the operating conditions of the alkylation unit are as follows: the feed flow rate for the single reactor is at around 30−70 tons/h; the reactor inlet temperature is at about 2.0−4.0 °C; the reactor outlet temperature is at around 6.0−6.5 °C; the ratio of isobutane to olefins (molar ratio) at the reactor inlet is between 7:1 and 12:1; the acid-to-hydrocarbon ratio (volume ratio) inside the reactor is around 1.1; and the acid concentration (wt %) of the three reactors is roughly around 92−96%. The reactor pressure is maintained at about 0.48 MPa, which is to keep the liquid phase of reactants and has no other effect on the alkylation reaction. The reactor volume of the industrial alkylation unit is 48.41 m^3, in which the volume of the space between the hydrocarbon phase inlet and the reactor outlet including the draft tube and agitation area is 24.86 m^3. It is considered as the reaction zone in the model since no olefins are present at the reactor outlet. Also, the olefins are completely converted in the reaction zone. In industrial production, the gas chromatograph with an Al_2O_3 (PLOT) chromatographic column and hydrogen flame ionization detector was used to identify and quantify all components.

Analyzing the influences of feed flow rate, acid-to-hydrocarbon ratio, acid concentration, the ratio of isobutane to olefins, reaction temperature, and other factors on the distribution of alkylation products and properties such as octane number, it is found that the feedstock feed rate had a greater effect on the distribution and properties of the products than other factors.

Figure 3 shows the effect of the total feedstock flow on the C_8 distribution and research octane number (RON) of the product from the three reactors. A message from the graph is that the selectivity of C_8 for the alkylation reaction becomes worse as the feed load increases, which is very important for kinetic modeling.

3. KINETIC MODEL

3.1. Lumped Model and Reaction Network. The main alkylation reaction is the addition reaction of isobutane and olefins. The commonly used catalysts for alkylation reactions are sulfuric acid, hydrofluoric acid, alumina, and so on. The sulfuric acid catalyst is used in this device. From the composition of the alkylation reaction products, alkylation reactions are complex and involve not only the main reaction but also many side reactions: isomerization, polymerization, cracking, and so forth. Thus, in the study of kinetics, the compounds in the complicated reaction system can be divided into several pseudo-components, or lumps, based on the principle that their kinetic properties are similar. Therefore, the reaction network is simplified which is facilitated to the kinetic study of the complex reaction system.[24]

https://doi.org/10.1021/acsomega.1c06850
ACS Omega 2022, 7, 9513−9526

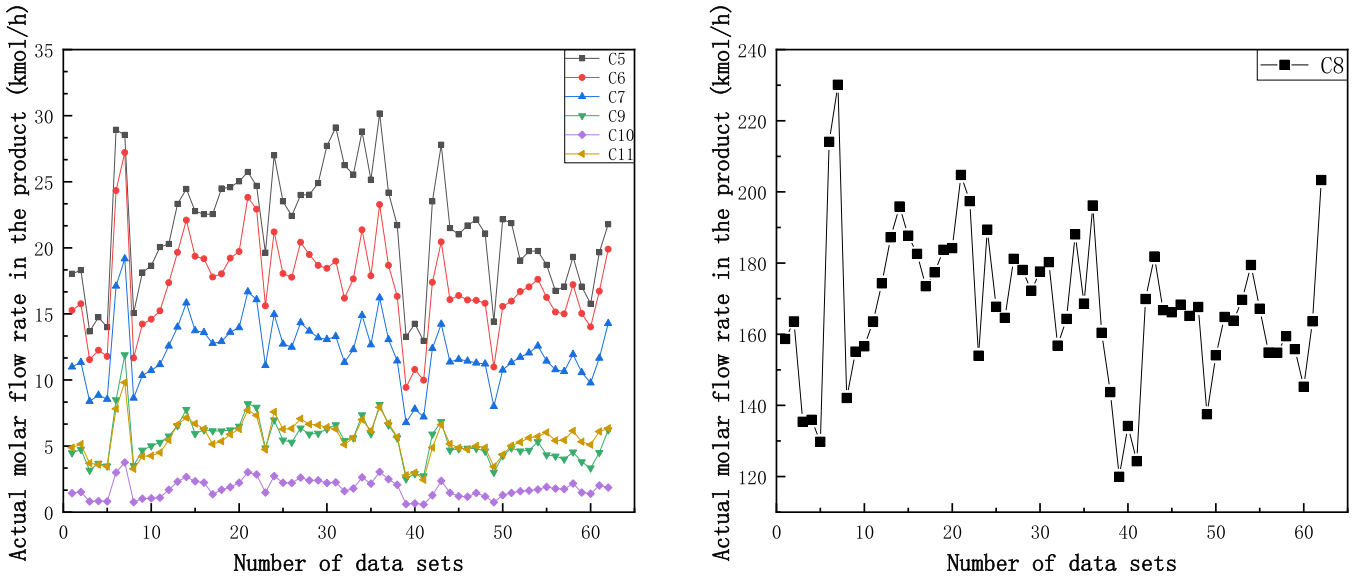

Figure 4. Molar flow rate of byproducts (left) and main products (right).

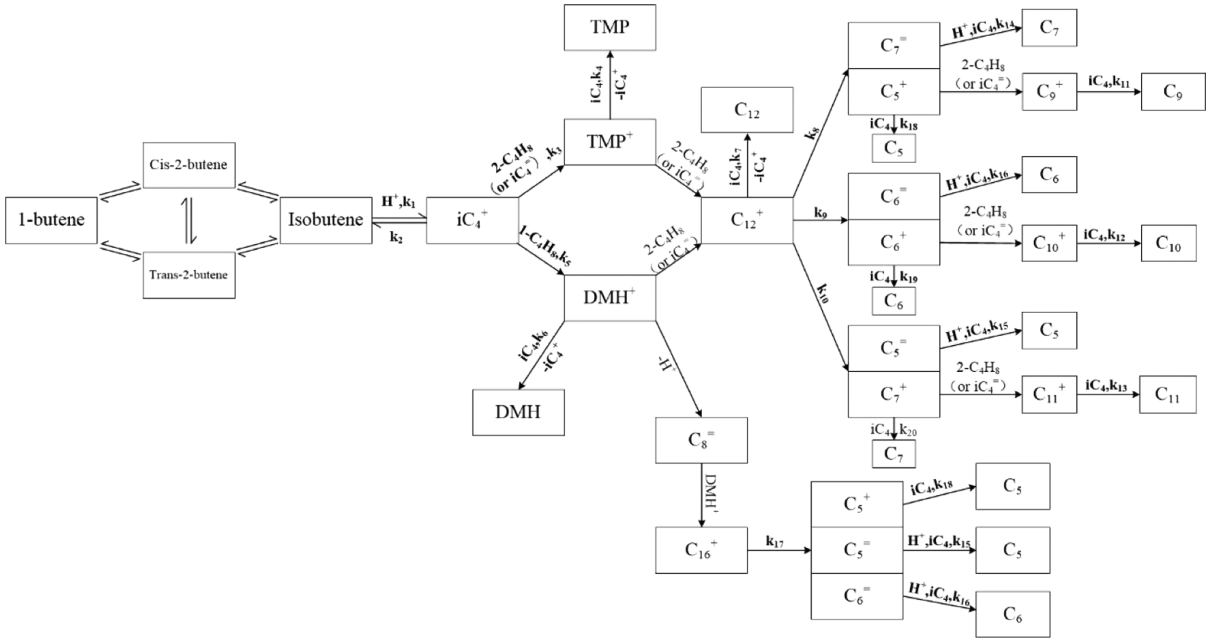

Figure 5. Reaction network.

According to the daily analysis from the refinery, the reaction products (except carbon eight) are classified by carbon numbers, which are C_5, C_6, C_7, C_9, C_{10}, and C_{11}, respectively. Considering that the reaction of isobutane with different butenes may give different alkanes, C_8 is divided into two lumps according to the chain length: TMP and DMH.

Daily industrial data from the commercial alkylation unit show that the raw materials for the alkylation reaction are olefins and isobutane, with a small amount of isopentane. In the raw materials, there are also some diluents, also known as inert components, respectively, propane and *n*-butane, which are not involved in the reaction, so they are not considered in the model. However, it should be noted that their content will affect the relative concentration of butene and isobutane due to their dilution effect.

With the continuous exploration of the mechanism of the alkylation reaction, it is well-accepted that the alkylation follows the classic carbonium ion mechanism.[25,26] The alkylation products are produced by a chain reaction mechanism, which consists of three processes: chain initiation, chain growth, and chain termination.

First, in the alkylation reaction with sulfuric acid as catalyst, the hydrogen proton dissociated from sulfuric acid reacts with isobutene to form the *tert*-butyl carbon cation, which is the chain initiation process. Then, the *tert*-butyl carbon cation adds to the butene molecule to form the C_8 carbon cation, which is the chain growth process. After that, the C_8 carbon cation follows the hydrogen transfer reaction with isobutane to produce isooctane and regenerate the *tert*-butyl carbon cation, which is the chain termination process.

https://doi.org/10.1021/acsomega.1c06850
ACS Omega 2022, 7, 9513−9526

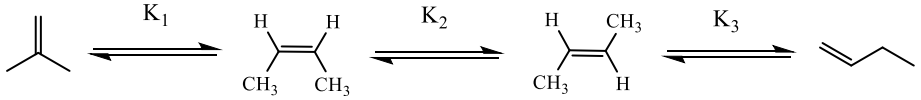

Figure 6. Isomerization reaction between olefins.

At the same time, the C_8 carbon ion may also undergo an addition reaction with olefins to form the C_{12} carbon cation, which is then cracked to form the lighter carbon cation and the corresponding lighter olefin.[27] This can be used to explain part of the light hydrocarbon formation, but based on the analysis of the products, this is far from sufficient.

Figure 4 shows that the molar flow rate of light hydrocarbons (C_5−C_7) is greater than the molar flow rate of heavy hydrocarbons (C_9−C_{11}). To be specific, the molar flow rate of C_5 is slightly smaller than the molar flow rate of C_6 and they are both greater than the molar flow rate of C_7 alkanes. The molar flow rate of C_9 and C_{11} alkanes is approximately the same in the products, and the molar flow rate of C_{10} is about 1/3 of the molar flow rate of C_{11}. This result suggests that it is not reasonable to treat the light hydrocarbons (C_5−C_7) as being produced only by the cracking reaction of C_{12}^+ because the creaking reaction of C_{12}^+ is equimolar, which is not consistent with the actual results. Therefore, it is necessary to add further information on the mechanism of light hydrocarbon generation.

Albright and Doshi[28] described the degradation and isomerization reactions of isobutane and light hydrocarbons and speculated on the most likely mechanism of DMH^+ degradation. DMH^+ and dimethylhexenes (formed from DMH^+) react to generate C_{16}^+, which eventually undergoes a cracking reaction to form small-molecule degradation products.

Based on the abovementioned discussion and analysis, the reaction network of alkylation reaction is proposed, as shown in Figure 5.

3.2. Reaction Kinetic Equation. Based on the reaction network mentioned above, the obtained reaction rate equations are shown in Table A1.

In the alkylation process, TMP^+ or DMH^+ is produced by a chain reaction in which iC_4^+ adds to a butene molecule to form C_8^+, followed by the hydrogen transfer reaction from isobutane to form TMP or DMH and regenerate the iC_4^+. C_{12}^+ is fragmented to smaller isoalkyl cations and olefins.[18] Usually, the fragmentation position is near the middle of the chain, and the probability of fragmentation at the side is smaller, which is proved by the product analysis that the mass of C_3 did not change much when making material balance. Based on actual industrial data, considering that 1-butene, *cis*-2-butene, *trans*-2-butene, and isobutene are controlled by chemical equilibrium, olefins can be regarded as a lump, and the concentration of different olefins within the butene lump can be calculated using the equilibrium constant.[29]

Figure 6 shows the isomerization reactions between the four olefins.

If $C_{4,n}$, $C_{4,c}$, $C_{4,t}$, and $C_{4,i}$ are used to, respectively, represent the concentrations of 1-butene, *cis*-2-butene, *trans*-2-butene, and isobutene and C_4 represents the concentration of lumped butene, then

$$C_{4,n} = \alpha \cdot C_4 \tag{1}$$

$$C_{4,c} = \beta \cdot C_4 \tag{2}$$

$$C_{4,t} = \gamma \cdot C_4 \tag{3}$$

$$C_{4,i} = (1 - \alpha - \beta - \gamma) \cdot C_4 \tag{4}$$

where

$$\alpha = \frac{1}{1 + K_1 + K_2 \cdot K_1 + K_3 \cdot K_2 \cdot K_1} \tag{5}$$

$$\beta = \frac{K_1}{1 + K_1 + K_2 \cdot K_1 + K_3 \cdot K_2 \cdot K_1} \tag{6}$$

$$\gamma = \frac{K_2 \cdot K_1}{1 + K_1 + K_2 \cdot K_1 + K_3 \cdot K_2 \cdot K_1} \tag{7}$$

4. REACTOR MODEL

According to the introduction of the alkylation unit, it can be found that three horizontal flow reactors are used in the alkylation process, and each of which is matched with an acid settler. The flow of the hydrocarbon phase in each reactor is parallel. The acid phase is circulated between the reactor and the acid settler to maintain the volume ratio of acid to hydrocarbon in the reactor, where the catalyst in the first and second reactors is supplemented with a little fresh acid, while the catalyst in the third reactor is supplemented with a little acid from the first and second acid settlers.

When the acid and hydrocarbon materials enter the reactor inlet, the stirring impeller will rapidly disperse the hydrocarbon phase into the sulfuric acid catalyst to form an acid−hydrocarbon emulsion, which will be discharged from the other side of the impeller and enter the sealing side along with the space between the draft tube and the reactor shell under the influence of the hydraulic head, part of which flows into the acid settler as a reaction product along the rising line and the other part returns to the draft tube to form a cycle in the reactor. The fluid flow state in the alkylation reactor[23] is shown in Figure 2.

For the industrial alkylation reactor, the flow pattern inside the reactor cannot be measured directly, and it is difficult to build the reactor model accurately when only the reactor operating conditions and the content of each component are known. Cai and Dai[30] performed CFD analysis of the alkylation reactor using a standard k−ε model to investigate the relationship between the circulating flow rate, the impeller speed, and the impeller diameter in the reactor. By calculating the flow field at different operating speeds, it is found that the circulating flow rate in the draft tube is proportional to the rotational speed of the impeller, which is not frequently adjusted under normal operating conditions, so it can be assumed that the circulation flow rate in the draft tube is a fixed value.

In this way, according to the flow state of the fluid in the reactor and the structure pattern of the reactor, the reactor can be simplified to a plug flow reactor with circulation, and its structure is shown in Figure 7.

Alkylation reactions using sulfuric acid as catalyst are relatively complicated heterogeneous reactions that involve diffusion and chemical reaction. In order to simplify the model reasonably, the following assumptions are made:

https://doi.org/10.1021/acsomega.1c06850
ACS Omega 2022, 7, 9513−9526

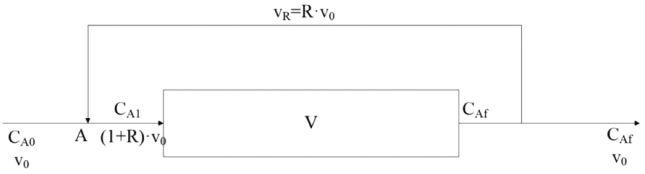

Figure 7. Reactor model.

(a) The reactor operates under constant pressure (0.48 MPa) and steady-state conditions.
(b) The flow model of the hydrocarbon and acid phases in the reactor is handled as PFR with circulation, and since the alkylation reaction is very fast and no olefins are found at the reactor outlet according to the daily analysis, the reaction is finished before reaching the reactor outlet and the circulation part does not involve the alkylation reaction.
(c) The circulating flow in the reactor is proportional to the speed of the stirring impeller, and due to the high-speed rotation of the stirring impeller in the reactor, the chemical reaction can be considered as the rate-determining step.
(d) According to the DCS data, the outlet temperature of each reactor does not change much, and there will be a large circulation flow inside the reactor to quickly remove the heat released from the alkylation reaction inside the reactor, which will make the temperature difference inside the reactor not change considerably, so the alkylation reactor is supposed to be an isothermal reactor.
(e) The residence time of the hydrocarbon phase in the reactor depends on the ratio of acid to hydrocarbon, feed flow rate, and circulating flow rate in the draft tube.

Based on the reaction network and assumptions, the model can be calculated using the following eqs 8−27.

$$\frac{dc_1}{d\tau} = (-r_1 + r_2 - r_3{\cdot}f(\mathrm{AO}, w\mathrm{cor}) - r_5{\cdot}f(\mathrm{AO}, w\mathrm{cor}) - r_7 - r_8 - r_9 - r_{10} - r_{11} - r_{12} - r_{13})\cdot\mathrm{AO}\cdot w \quad (8)$$

$$\frac{dc_2}{d\tau} = (r_3{\cdot}f(\mathrm{AO}, w\mathrm{cor}) - r_4{\cdot}f(\mathrm{AO}, w\mathrm{cor}) - r_7 - r_8 - r_9 - r_{10})\cdot\mathrm{AO}\cdot w \quad (9)$$

$$\frac{dc_3}{d\tau} = (r_5{\cdot}f(\mathrm{AO}, w\mathrm{cor}) - r_6{\cdot}f(\mathrm{AO}, w\mathrm{cor}) - r_{17})\cdot\mathrm{AO}\cdot w \quad (10)$$

$$\frac{dc_4}{d\tau} = (-r_4{\cdot}f(\mathrm{AO}, w\mathrm{cor}) - r_6{\cdot}f(\mathrm{AO}, w\mathrm{cor}) - r_7 - r_{11} - r_{12} - r_{13} - r_{14} - r_{15} - r_{16} - r_{18} - r_{19} - r_{20})\cdot\mathrm{AO}\cdot w \quad (11)$$

$$\frac{dc_5}{d\tau} = (r_{15} + r_{18})\cdot\mathrm{AO}\cdot w \quad (12)$$

$$\frac{dc_6}{d\tau} = (r_{16} + r_{19})\cdot\mathrm{AO}\cdot w \quad (13)$$

$$\frac{dc_7}{d\tau} = (r_{14} + r_{20})\cdot\mathrm{AO}\cdot w \quad (14)$$

$$\frac{dc_8}{d\tau} = r_4{\cdot}f(\mathrm{AO}, w\mathrm{cor})\cdot\mathrm{AO}\cdot w \quad (15)$$

$$\frac{dc_9}{d\tau} = r_{11}\cdot\mathrm{AO}\cdot w \quad (16)$$

$$\frac{dc_{10}}{d\tau} = r_{12}\cdot\mathrm{AO}\cdot w \quad (17)$$

$$\frac{dc_{11}}{d\tau} = r_{13}\cdot\mathrm{AO}\cdot w \quad (18)$$

$$\frac{dc_{12}}{d\tau} = r_7\cdot\mathrm{AO}\cdot w \quad (19)$$

$$\frac{dc_{13}}{d\tau} = r_6{\cdot}f(\mathrm{AO}, w\mathrm{cor})\cdot\mathrm{AO}\cdot w \quad (20)$$

$$\frac{dc_{14}}{d\tau} = (r_1 - r_2 - r_3{\cdot}f(\mathrm{AO}, w\mathrm{cor}) + r_4{\cdot}f(\mathrm{AO}, w\mathrm{cor}) - r_5{\cdot}f(\mathrm{AO}, w\mathrm{cor}) + r_6{\cdot}f(\mathrm{AO}, w\mathrm{cor}) + r_7 + r_{11} + r_{12} + r_{13} + r_{14} + r_{15} + r_{16} + r_{18} + r_{19} + r_{20})\cdot\mathrm{AO}\cdot w \quad (21)$$

$$\frac{dc_{15}}{d\tau} = (r_8 - r_{11} + r_{17} - r_{18})\cdot\mathrm{AO}\cdot w \quad (22)$$

$$\frac{dc_{16}}{d\tau} = (r_9 - r_{12} - r_{19})\cdot\mathrm{AO}\cdot w \quad (23)$$

$$\frac{dc_{17}}{d\tau} = (r_{10} - r_{13} - r_{20})\cdot\mathrm{AO}\cdot w \quad (24)$$

$$\frac{dc_{18}}{d\tau} = (r_{10} - r_{15} + r_{17})\cdot\mathrm{AO}\cdot w \quad (25)$$

$$\frac{dc_{19}}{d\tau} = (r_9 - r_{16} + r_{17})\cdot\mathrm{AO}\cdot w \quad (26)$$

$$\frac{dc_{20}}{d\tau} = (r_8 - r_{14})\cdot\mathrm{AO}\cdot\mathrm{w} \quad (27)$$

where c_j (j = 1−20) denotes the concentration of each lumped component, which are, respectively, butene, TMP^+, DMH^+, isobutane, C_5, C_6, C_7, TMP, C_9, C_{10}, C_{11}, C_{12}, DMH, iC_4^+, C_5^+, C_6^+, C_7^+, $C_5^=$, $C_6^=$, and $C_7^=$; AO is the acid-to-hydrocarbon ratio; w is the concentration(wt %) of sulfuric acid; and f(AO,$w$cor) is a correction function introduced for the main reaction;

In actual alkylation industrial production, the operating conditions are relatively homogeneous, and the variation range of acid concentration and the acid-to-hydrocarbon ratio are small. However, large variations in acid concentration and acid-to-hydrocarbon ratio can have a significant effect on the distribution of reaction products and RON.

In the alkylation process, the concentration of sulfuric acid is strictly controlled as an important operating variable. The impurities[31] affecting sulfuric acid concentration are generally divided into two types: water and acid-soluble hydrocarbons.[32,33] The presence of water facilitates the dissociation of sulfuric acid and provides the H^+ required for the alkylation reaction, and acid-soluble hydrocarbons are also highly ionized, which can make isobutene into the *tert*-butyl carbon cation and induce the alkylation reaction. The abovementioned is the favorable side of impurities, but an increase in the concentration of either water or acid-soluble hydrocarbons causes the sulfuric acid concentration to decrease and the unfavorable side

https://doi.org/10.1021/acsomega.1c06850
ACS Omega 2022, 7, 9513−9526

Table 1. Kinetic Parameters of the Model with 95% Confidence Intervals[38a]

reaction rate constant	numerical value	reaction rate constant	numerical value
k_1 (min^{-1})	11.63 ± 3.58	k_{11} ($kg^2\ mol^{-2}\ min^{-1}$)	86.89 ± 19.32
k_2 (min^{-1})	16.44 ± 4.62	k_{12} ($kg^2\ mol^{-2}\ min^{-1}$)	22.82 ± 6.05
k_3 ($kg\ mol^{-1}\ min^{-1}$)	862.37 ± 187.20	k_{13} ($kg^2\ mol^{-2}\ min^{-1}$)	90.22 ± 27.73
k_4 ($kg\ mol^{-1}\ min^{-1}$)	1.54 ± 0.26	k_{14} ($kg\ mol^{-1}\ min^{-1}$)	14.28 ± 3.61
k_5 ($kg\ mol^{-1}\ min^{-1}$)	12956.94 ± 4072.1	k_{15} ($kg\ mol^{-1}\ min^{-1}$)	4.56 ± 1.24
k_6 ($kg\ mol^{-1}\ min^{-1}$)	0.2187 ± 0.11	k_{16} ($kg\ mol^{-1}\ min^{-1}$)	51.22 ± 17.54
k_7 ($kg^2\ mol^{-2}\ min^{-1}$)	1.36 ± 0.34	k_{17} ($kg\ mol^{-1}\ min^{-1}$)	3521.91 ± 797.47
k_8 ($kg\ mol^{-1}\ min^{-1}$)	89.41 ± 16.49	k_{18} ($kg\ mol^{-1}\ min^{-1}$)	1.28 ± 0.16
k_9 ($kg\ mol^{-1}\ min^{-1}$)	90.67 ± 9.60	k_{19} ($kg\ mol^{-1}\ min^{-1}$)	2.06 ± 0.73
k_{10} ($kg\ mol^{-1}\ min^{-1}$)	119.86 ± 20.33	k_{20} ($kg\ mol^{-1}\ min^{-1}$)	3.71 ± 0.96

[a]Note: all values of the reaction rate constants are greater than 0.

reactions are strengthened.[34] The increase in water makes the corrosion ability of sulfuric acid enhanced, while the increase in acid-soluble hydrocarbons may increase the viscosity of acid, and these have important effects on the distribution of alkylation products.

Also, the acid-to-hydrocarbon ratio is also a very important variable. In the reactor, the acid phase and hydrocarbon phase form an emulsion phase under the high-speed agitation of the impeller. If the acid−hydrocarbon ratio is relatively small, it cannot make the acid become a continuous phase, which increases the generation of byproducts and leads to poor quality of the generated alkylates and high acid consumption.

In general, when the sulfuric acid concentration reaches 95−96%, the performance of sulfuric acid-catalyzed alkylation reaction is the best, which is beneficial to the generation of main alkylation products and can improve the octane number of products. In addition, the lower acid concentration and acid-to-hydrocarbon ratio will favor the alkylation side reactions and reduce the selectivity of C_8 main reactions. The reason may be that some macromolecules will be generated in the side reaction, such as the reaction of some olefins and sulfuric acid to form sulphate;[35] it may also intensify the olefin polymerization reaction and increase the HEs in the alkylation products, and these results will lead to the lower octane number of the alkylates. Therefore, a correction function[36] for the main reaction is introduced in the model to reflect the influence of the change in acid concentration and acid−hydrocarbon ratio on the selectivity of the main reaction. The type of the correction function is as follows.

$$f(\mathrm{AO}, w\mathrm{cor}) = \mathrm{AO}\cdot e^{w\mathrm{cor}} \tag{28}$$

where AO is the ratio of acid to hydrocarbon and $w$cor is the coefficient after renormalizing the acid concentration, which can more clearly reflect the influence of acid concentration on C_8 selectivity.

Lee and Harriott[18] studied the acid-catalyzed reaction of isobutane with 1-butene and the 1-butene oligomerization. It is found that the rate constant for isobutane with 1-butene goes up as the acid strength increases. However, in this paper, there are no such reaction steps that correspond exactly to the reaction in the literature. Even so, it can be found that the chain growth and chain termination reaction steps of the main reactions in our model are similar to the alkylation reaction of isobutane with 1-butene. Therefore, it is reasonable to correct the reaction rate of the main reaction by adjusting the acid concentration and the acid-to-hydrocarbon ratio.

5. PARAMETER ESTIMATION

To ensure the reliability of the kinetic parameters, most of the data (52 sets) are needed for parameter estimation. Left data (10 sets) with quite different conditions are selected to validate the reliability and adaptability of the model. The variation range of component concentrations and operating conditions are shown in Figure A1.

Based on the kinetic model mentioned above, the model has 20 reaction rate constants, one circulating flow rate and three equilibrium constants between olefins. Thermodynamically, K_1, K_2, and K_3 are a function of temperature and can be calculated using the Gibbs free energy of the isomerization reaction between olefins. In this paper, the REquil module in Aspen plus is used to calculate the chemical equilibrium and obtain the equilibrium constants K_1, K_2, and K_3. The equilibrium constants K_1, K_2, and K_3 were 9.207, 2.636, and 9.248 at 279.2 K, respectively. Therefore, the values of α, β, and γ can be calculated as 0.0038, 0.0354, and 0.0934, respectively.

For the calculation of the circulation flow rate in the reactor, when fitting the parameters based on the actual data, it was found that when the circulation flow rate was larger, that is, when the reactor model was closer to the CSTR model, the trend of the calculated reaction product concentration and the fresh feed flow rate was opposite to the actual trend. Therefore, considering to reduce the fitting error, the value of the circulation flow rate was determined by minimizing the absolute deviation.

To estimate rate constants in eqs 8−27, the nonlinear least-squares fitting method was used with the following object function

$$Q = \sum_{j=1}^{n}\sum^{z}(x_{j,\mathrm{exp}} - x_{j,\mathrm{cal}})^2 \tag{29}$$

where $x_{j,\mathrm{exp}}$ and $x_{j,\mathrm{cal}}$ represent the measured value and model calculation value of component j at the outlet of the reactor, respectively; z denotes the number of lumps; and n represents the number of sets of data. In this work, the Isqnonlin function in Matlab is used to estimate k_1−k_{20}, which is based on the principle of minimizing the sum of squares of errors. The Gear method with variable step size and order is used to solve the stiff kinetic differential equations.[37] It should be noted that there are three reactors with different acid and hydrocarbon concentrations, and therefore, each reactor needs to be calculated separately when performing the numerical analysis, and then, the results of the three reactors are mixed and compared with the actual values.

https://doi.org/10.1021/acsomega.1c06850
ACS Omega 2022, 7, 9513−9526

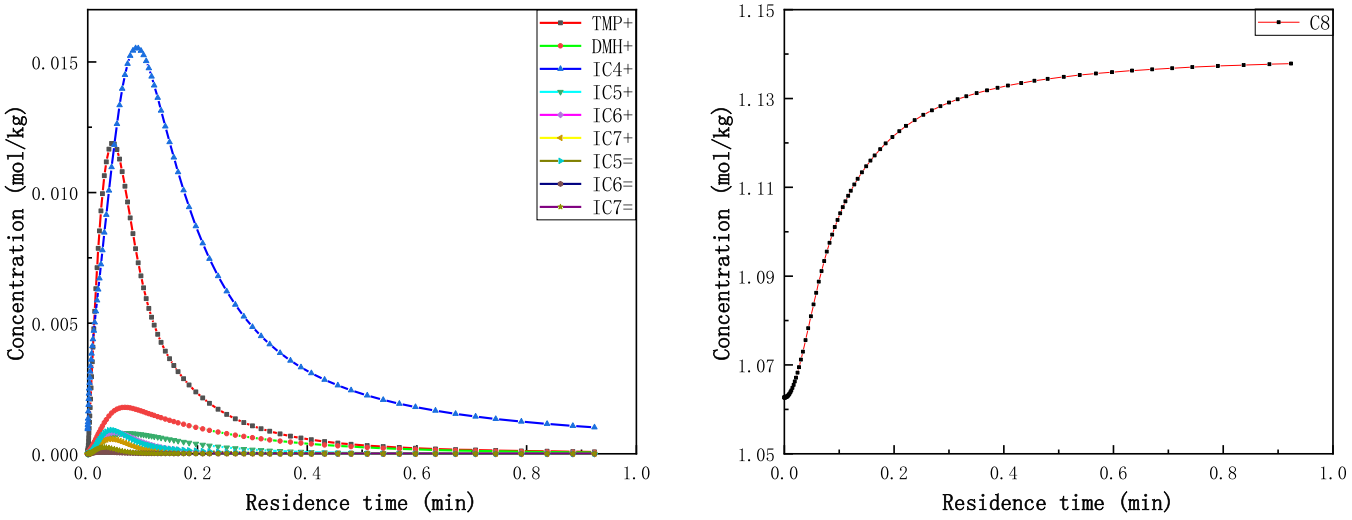

Figure 8. Trend of carbonium ion (left) and C8 (right) along the reactor.

All substances involved in the alkylation reaction, including propane, *n*-butane, olefins, and isobutane, are shown in Appendix A. 2. In the fresh feed, there is no dissociation of the catalyst and therefore no intermediate components are present, so the initial concentrations of all components except butene and isobutane are 0 mol/kg. Moreover, according to the data of the industrial plant, the concentration of olefins at the reactor exit is almost 0 mol/kg, so it can be assumed that the olefins are completely converted in the reactor. This is also in accordance with the feature that the alkylation reaction is fast and is completely converted before the reactor exit.

When solving the reactor model, it is assumed that the composition of the circulating flow stream is initially the same as that of the fresh feed, and the outlet stream after each calculation will be circulated partly back to the reactor inlet until the relative deviation of the outlet composition of two consecutive calculations does not exceed 1%, which can be considered as iterative convergence, and its value can be regarded as the reactor outlet concentration.

In this work, 52 sets of data from the alkylation unit are used to estimate the kinetic parameters in the model, using nonlinear least squares to minimize the objective function. The results obtained using nonlinear least squares are shown in Table 1.

It can be seen from the abovementioned table that the reaction rates for chain growth are much larger than those for chain initiation and chain termination, which are particularly prominent in the TMP^+ and DMH^+ production. From the point of view of the chain reaction mechanism, it is a very normal phenomenon that the alkylation reaction rate increases after the chain initiation process due to the continuous accumulation of iC_4^+. In the chain termination stage, the reaction rate decreases because of the decrease in olefins.

Since the data were collected from an industrial unit, there was inevitably more deviation in the data collection and analysis process compared with experimental kinetic investigation in the laboratory. As shown in Table 1, almost all confidence intervals are one magnitude smaller than their own parameters, which confirms the reliability of the estimated rate constants.

It can also be found that the subsequent reaction rate of DMH^+ is large. From the analysis of the products, the light hydrocarbons are not only produced by the crack of C_{12}^+ but also by the subsequent reaction of DMH^+ to produce C_5 and C_6 alkanes. This reaction rate will affect the distribution of C_5 and C_6 in the product.

The value of the circulating flow rate inside the reactor is about 425 tons/h, which is about 10 times the flow rate of fresh feed to the reactor. The alkylation reaction is an exothermic reaction; the heat released by the reaction is quite large. In order to remove the heat, it is necessary to form a large flow circulation inside the reactor.

According to the abovementioned kinetic model of the alkylation reaction, the reaction kinetic model was solved by the Gear method of solving a rigid system of differential equations, and the average relative deviations of C_5, C_6, C_7, C_8, C_9, C_{10}, and C_{11} in alkylates were calculated as 9.24, 5.42, 4.66, 1.84, 8.72, 21.20, and 8.49%, respectively. The fitting effect of the main alkylation product is good, and the relative deviation for the byproducts is relatively large, which is due to the proportion of byproducts in the alkylation product being small especially the C_{10} hydrocarbons. In general, the data of the model fit well, indicating that the established kinetic model based on the classic carbonium ion mechanism is relatively reasonable.

6. MODEL VERIFICATION

In order to verify the reliability of the established kinetic model and its kinetic parameters, prediction calculations should be performed with additional industrial data, and the reliability of the model can be judged by the degree of agreement between the predicted values and actual values. In this paper, 10 left sets of data from the alkylation unit with different reaction conditions and feedstock compositions were selected for validation calculation of alkylation product distribution.

The range of the feed flow rate selected in the validation is approximately about 35−60 tons/h. The relative deviations of C_5, C_6, C_7, C_8, C_9, C_{10}, and C_{11} were 12.78, 5.32, 5.36, 1.95, 25.51, 17.72, and 10.98%, respectively. The relative deviations indicate that the kinetic model and kinetic parameters are reliable and can achieve accurate product distribution prediction for industrial alkylation plants.

7. MODEL PREDICTION

In actual industrial production, the product distribution and product quality may be influenced by inert components, the ratio of isobutane to olefins, the flow rate of reaction feedstock,

https://doi.org/10.1021/acsomega.1c06850
ACS Omega 2022, 7, 9513−9526

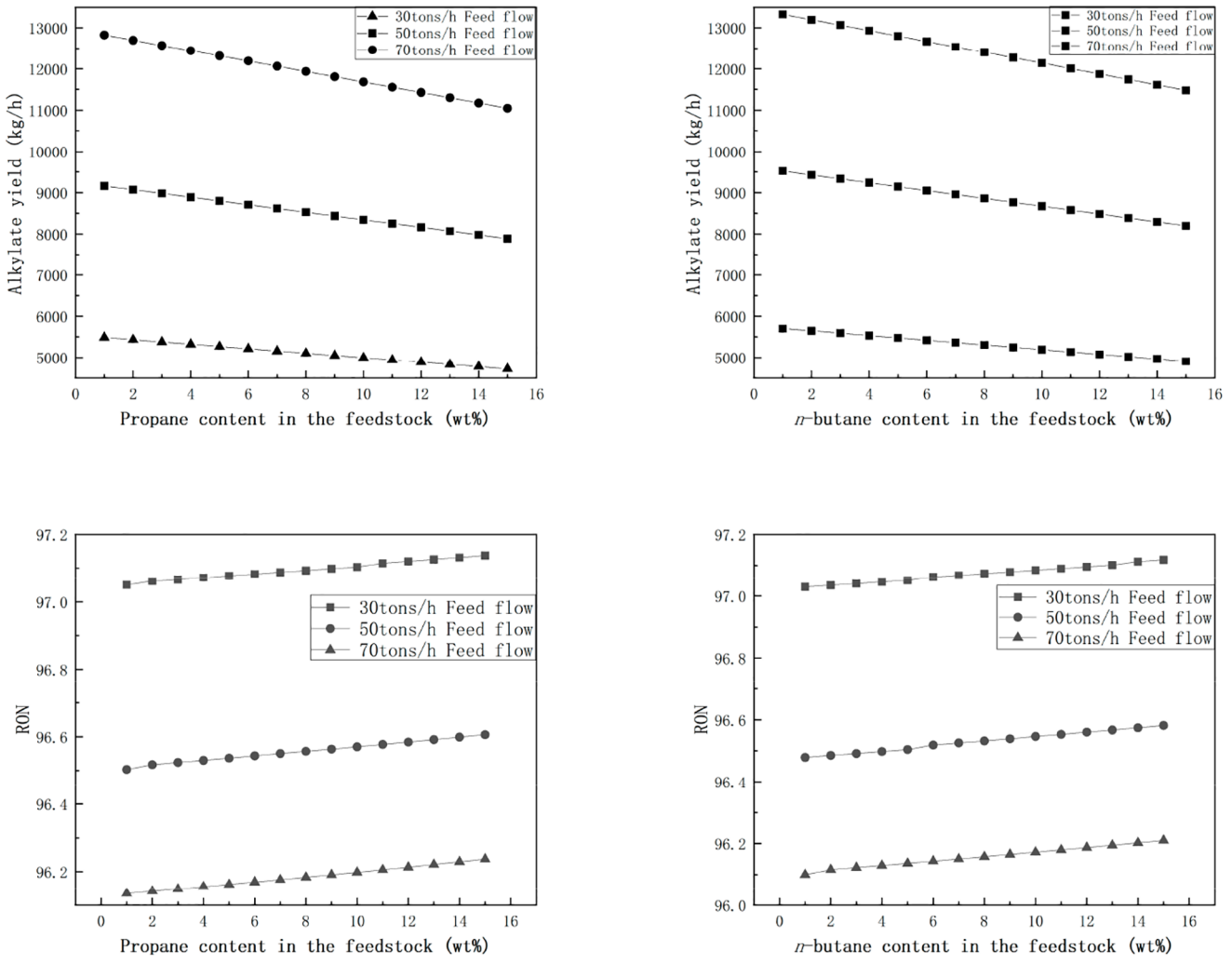

Figure 9. Influence of the impurities in the feedstock on alkylate yield and RON at different feed flows.

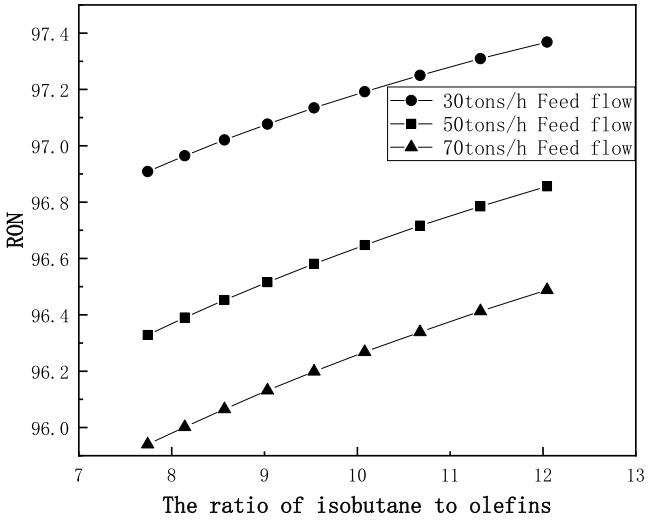

Figure 10. Influence of the ratio of isobutane to olefins on RON at different feed flows.

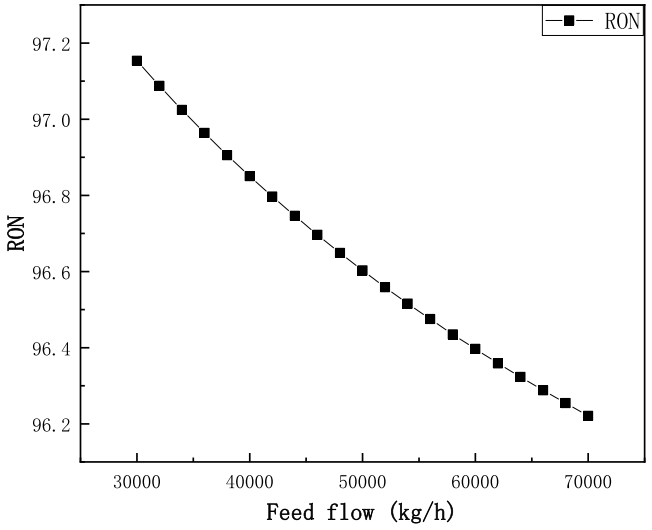

Figure 11. Influence of the feed flow rate on RON.

and so on. Based on the developed kinetic model of alkylation reaction using sulfuric acid as catalyst, the trend along the alkylation reactor and the effects of reaction conditions at different feed flows were studied.

7.1. Trend along with the Alkylation Reactor. Based on the abovementioned model parameters, the changes in material composition in each reactor can be predicted reliably. The concentration profiles of each intermediate and C_8 produced in

https://doi.org/10.1021/acsomega.1c06850
ACS Omega 2022, 7, 9513−9526

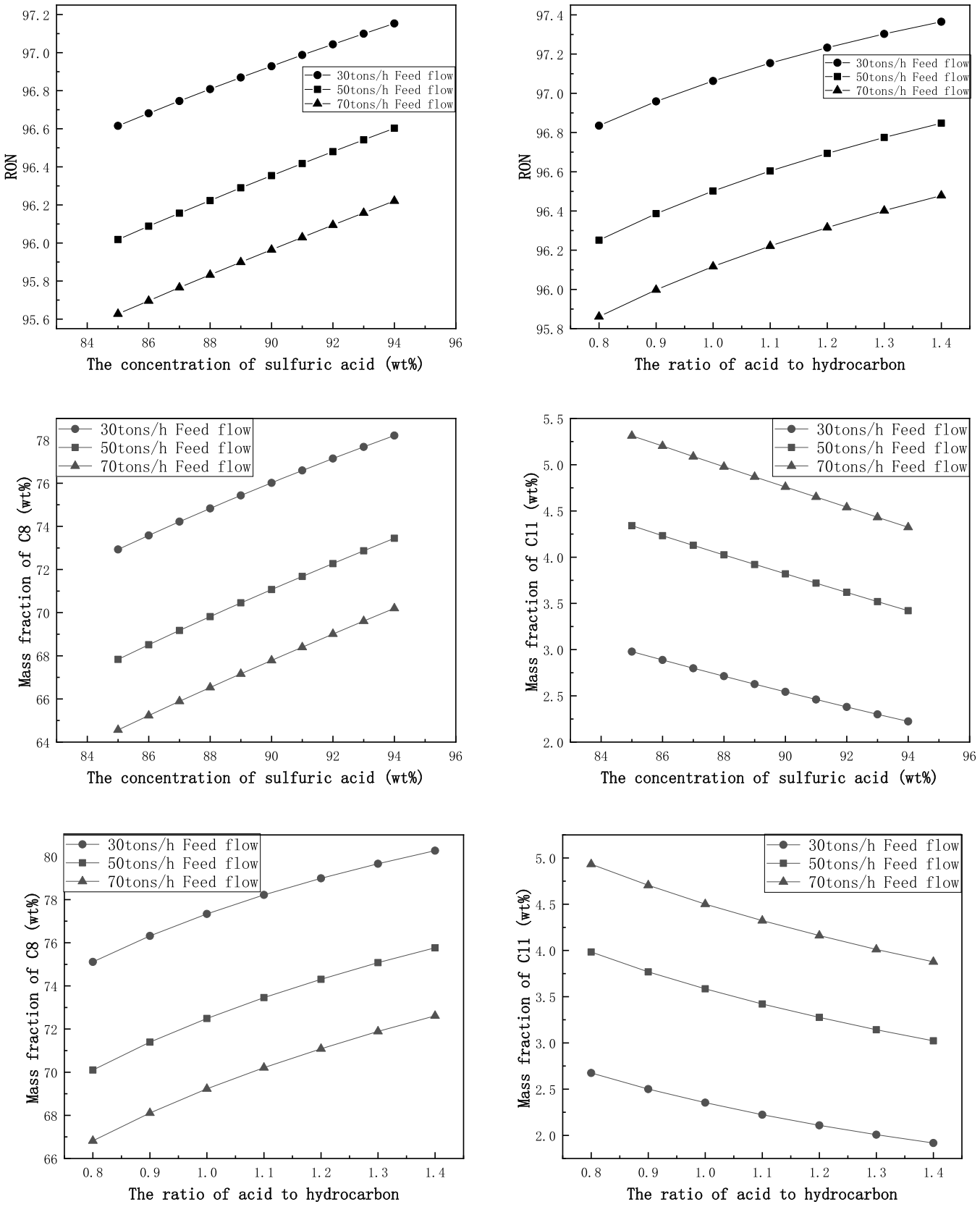

Figure 12. Influence of sulfuric acid on the mass fraction of C8 and C11 and RON at different feed flows.

the alkylation of isobutane with olefins are plotted in Figure 8. It shows that all the carbonium ions are created and lost quickly during alkylation. This demonstrates that the alkylation is a very rapid reaction. Almost after 0.5 min, each of the species reaches a platform individually.

In general, the residence time of alkylation reactors in the industry is about 5−20 min, which is the value of the whole

https://doi.org/10.1021/acsomega.1c06850
ACS Omega 2022, 7, 9513−9526

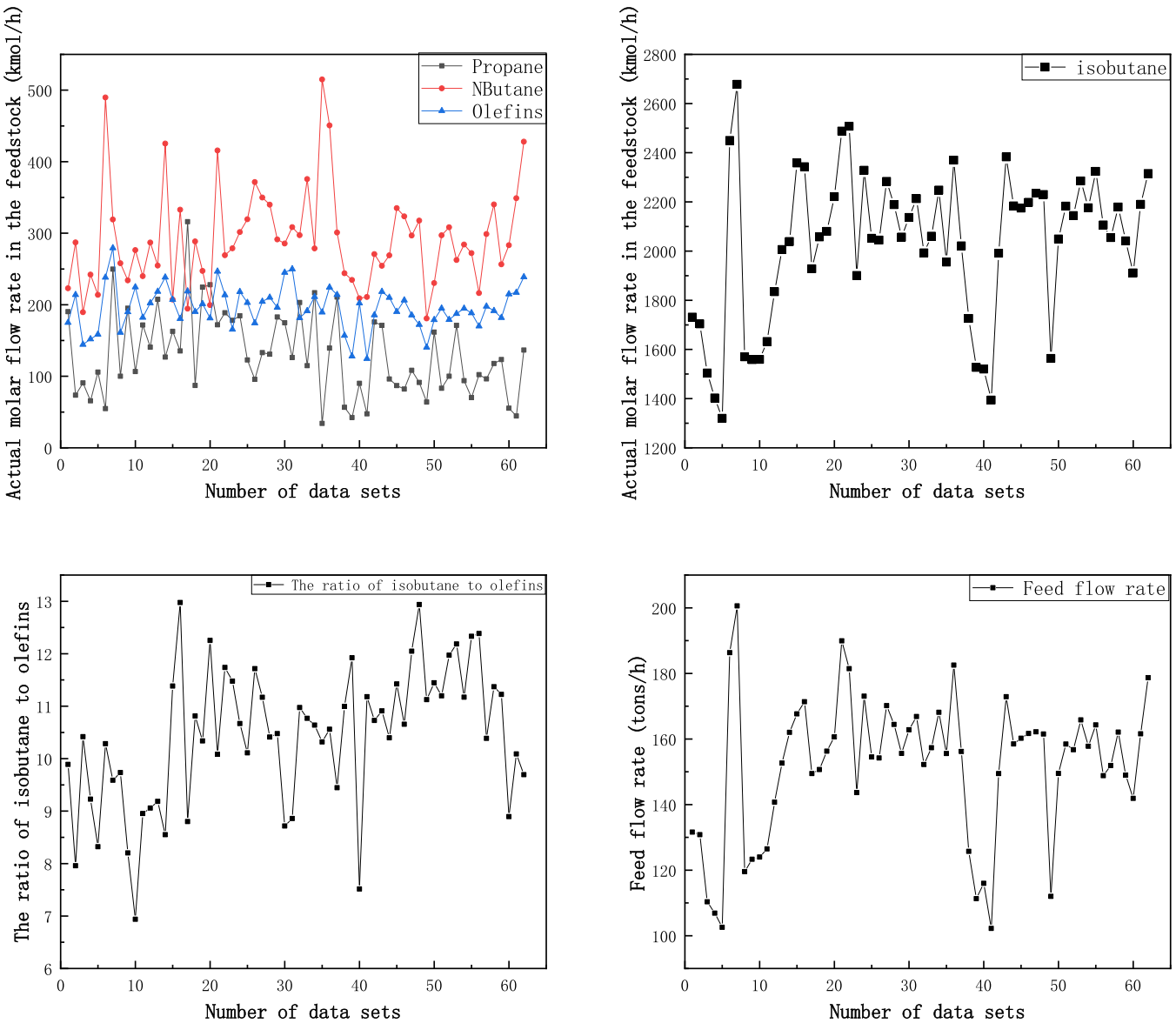

Figure A1. Variation range of material concentrations and operating conditions.

reactor volume divided by the volume flow rate of the fresh feed hydrocarbon. In this paper, the reaction zone includes only the draft tube and the agitation zone in the model, and its residence time is affected by the feed flow rate of fresh hydrocarbon, the flow rate of circulating hydrocarbon, and the ratio of acid to hydrocarbon. Since the circulation flow rate is about 10 times the fresh feed flow rate, the residence time is about 1 min.

7.2. Influence of the Propane and *n*-Butane Content in the Feedstock. The impurities in the feedstock are low-molecular alkanes that do not participate in the reaction. Based on the daily analysis data of the petrochemical industry, it is known that the low-molecular alkanes are mainly propane and *n*-butane, which can dilute the hydrocarbon phase and thus reduce the concentrations of isobutane and butene.

Figure 9 shows the effect of propane and *n*-butane in the feedstock on the quality of the alkylates at different feed flows.

Model calculation results show that the RON changed slightly when the propane and *n*-butane concentrations changed, but the alkylate yield changed significantly. This can be explained by the fact that propane and *n*-butane do not participate in the reaction in alkylation, and the increase in the concentration of these impurities reduces the yield of alkylates.

According to the model calculation results, the differences in the content of these dilution components are not significant and have a negligible effect on the octane number of alkylates within their variation range.

7.3. Influence of the Ratio of Isobutane to Olefins. During the alkylation process, this ratio is the molar ratio of isobutane to olefins in the feed hydrocarbon, and the reaction process is strongly influenced by the ratio. The ratio of each reactor can be adjusted by changing the flow rate of circulating isobutane. Daily analysis data from the plant shows that an addition of the molar ratio of isobutane and olefin in the feed hydrocarbon leads to the increase in the RON. In the simulation process, the effect of the ratio was investigated by keeping the respective reaction conditions such as feed flow rate, temperature, acid concentration, and acid-to-hydrocarbon ratio constant and adjusting the isobutane concentration at the reactor inlet to keep the alkene ratio varying in the range of 7−12.

https://doi.org/10.1021/acsomega.1c06850
ACS Omega 2022, 7, 9513−9526

Table A1. Reaction Rate Equations[a]

serial number	reaction rate equations
(1)	$r_1 = (1-\alpha-\beta-\gamma)\cdot k_1\cdot c_1$
(2)	$r_2 = k_2\cdot c_{14}$
(3)	$r_3 = (1-\alpha)\cdot k_3\cdot c_1\cdot c_{14}$
(4)	$r_4 = k_4\cdot c_2\cdot c_4$
(5)	$r_5 = \alpha\cdot k_5\cdot c_1\cdot c_{14}$
(6)	$r_6 = k_6\cdot c_3\cdot c_4$
(7)	$r_7 = (1-\alpha)\cdot k_7\cdot c_1\cdot c_2\cdot c_4$
(8)	$r_8 = (1-\alpha)\cdot k_8\cdot c_1\cdot c_2$
(9)	$r_9 = (1-\alpha)\cdot k_9\cdot c_1\cdot c_2$
(10)	$r_{10} = (1-\alpha)\cdot k_{10}\cdot c_1\cdot c_2$
(11)	$r_{11} = (1-\alpha)\cdot k_{11}\cdot c_1\cdot c_4\cdot c_{15}$
(12)	$r_{12} = (1-\alpha)\cdot k_{12}\cdot c_1\cdot c_4\cdot c_{16}$
(13)	$r_{13} = (1-\alpha)\cdot k_{13}\cdot c_1\cdot c_4\cdot c_{17}$
(14)	$r_{14} = k_{14}\cdot c_4\cdot c_{20}$
(15)	$r_{15} = k_{15}\cdot c_4\cdot c_{18}$
(16)	$r_{16} = k_{16}\cdot c_4\cdot c_{19}$
(17)	$r_{17} = k_{17}\cdot c_3\cdot c_3$
(18)	$r_{18} = k_{18}\cdot c_4\cdot c_{15}$
(19)	$r_{19} = k_{19}\cdot c_4\cdot c_{16}$
(20)	$r_{20} = k_{20}\cdot c_4\cdot c_{17}$

[a]Note: c_i (i = 1−20) denotes the concentration of each lumped component, which are, respectively, butene, TMP^+, DMH^+, isobutane, C_5, C_6, C_7, TMP, C_9, C_{10}, C_{11}, C_{12}, DMH, iC_4^+, C_5^+, C_6^+, C_7^+, $C_5^=$, $C_6^=$, and $C_7^=$ (mol/kg).

Figure 10 shows the effect of the ratio of isobutane to olefins on the RON of alkylates at different feed flows. Obviously, increasing the ratio is beneficial to obtain higher octane alkylates. According to the relevant literature,[39] the diffusion coefficient of butene is greater than that of isobutane. This means that butene is more likely to diffuse in sulfuric acid than isobutane, which leads to a phenomenon that butene at the interface or in sulfuric acid will be prone to a rapid polymerization reaction, which is not conducive to the generation of high-quality alkylated oil products. Therefore, maintaining a high isobutane concentration in the reactor is necessary to reduce the probability of collisions between olefins and to ensure the selectivity of the main alkylation reaction.

7.4. Influence of the Feed Flow Rate. During the alkylation process, the feed flow rate can be adjusted by changing the proportion of the mixed feed from the catalytic cracking unit to the alkylation unit. Small changes in the feed flow rate can change the residence time, but considering that the alkylation reaction is very rapid and the alkylation reactor is a PFR with circulation, the circulation flow rate is large than the fresh feed rate, so the change in residence time has less effect on the product distribution.

During the simulation, the temperature, hydrocarbon phase concentration, catalyst concentration, and acid-to-hydrocarbon ratio inside the reactor are kept constant, and only the feed rate is changed. The effect of the feed flow rate on the octane number of alkylates is shown in Figure 11.

It can be seen from the graph that as the feed flow rate increases, RON gets lower. The change in the feed flow rate is mainly due to the change in the ratio of isobutane to olefins of the reactor inlet, as iterative convergence is required for each reactor when calculating the reactor model. If the feed flow rate is different, the ratio of isobutane to butene after mixing will be different, which will affect the distribution of alkylation products.

7.5. Influence of Sulfuric Acid. Sulfuric acid, as a catalyst for the alkylation reaction, its concentration in the reactor and the volume ratio of it to hydrocarbon are very important parameters of the process. As mentioned above, for the alkylation reaction unit, the acid concentration in the first and second reactors is somewhat higher than that in the third reactor, which is around 92%.

In the prediction simulation, the reactor temperature, feed flow rate, and hydrocarbon phase concentration were kept constant, and the acid concentration and acid-to-hydrocarbon ratio were, respectively, varied to predict their effects on the product octane number, and the results are shown in Figure 12. Increasing the acid concentration and acid-to-hydrocarbon ratio can improve the selectivity of the alkylation reaction, so the octane number of the alkylated oil will be increased.

In general, maintaining a higher acid concentration is beneficial for alkylation reactions, and industrial production generally maintains the acid concentration at about 95% to obtain high-octane alkylate products. It is also very important to maintain a certain acid-to-hydrocarbon ratio in the reactor. Maintaining this ratio allows the acid to exist as a continuous phase and the hydrocarbon as a dispersed phase, which can reduce the probability of collision between olefins and inhibit the polymerization reaction.

8. CONCLUSIONS

(1) Based on the alkylation of isobutane with olefin carbonium ion mechanism, a kinetic model was developed for the actual alkylation reactor using sulfuric acid as a catalyst. The model parameters were regressed using industrial data, and the calculated values of the model and the actual data were in good agreement.

(2) According to the actual data of the normal operation of the oil refinery and the calculation results of the model, increasing the reaction feed flow will be conducive to the generation of byproducts (C_5−C_7 and C_9−C_{11}) and the decrease in RON.

APPENDIX A

Figure A1 and Table A1.

AUTHOR INFORMATION

Corresponding Author

Hongbo Jiang − *Research Institute of Petroleum Processing, East China University of Science and Technology, Shanghai 200237, China;* orcid.org/0000-0002-3025-682X; Phone: +86-21-64252816; Email: hbjiang@ecust.edu.cn

Authors

Zhicheng Xin − *Research Institute of Petroleum Processing, East China University of Science and Technology, Shanghai 200237, China*

Zhenyuan Zhang − *Petro-CyberWorks Information Technology Co., Ltd., Shanghai 200040, China*

Yushi Chen − *Petro-CyberWorks Information Technology Co., Ltd., Shanghai 200040, China*

https://doi.org/10.1021/acsomega.1c06850
ACS Omega 2022, 7, 9513−9526

Jianping Wang − *Petro-CyberWorks Information Technology Co., Ltd., Shanghai 200040, China*

Complete contact information is available at: https://pubs.acs.org/10.1021/acsomega.1c06850

Notes

The authors declare no competing financial interest.

NOMENCLATURE

T	temperature, K
P	pressure, MPa
i	the number of the reaction
j	the number of the component
r_i	rate of reaction i, mol kg^{-1} min^{-1}
k_i	rate constant of reaction i, kg^n mol^{-n} min^{-1}
c_j	the concentration of component j, mol kg^{-1}
R	circulation ratio in the reactor
C_{A0}	fresh material concentration at reactor inlet, mol m^{-3}
v_0	feed volume flow rate, m^3 h^{-1}
C_{A1}	material concentration after mixing of fresh feed with circulation stream, mol m^{-3}
V	reactor volume, m^3
v_R	circulation volume flow rate of the reactor, m^3 h^{-1}
C_{Af}	material concentration at reactor outlet, mol m^{-3}
α	conversion coefficient between 1-butene and lumped butene
β	conversion coefficient between *cis*-2-butene and lumped butene
γ	conversion coefficient between *trans*-2-butene and lumped butene
K_1	equilibrium constant of 1-butene and *cis*-2-butene
K_2	equilibrium constant of *cis*-2-butene and *trans*-2-butene
K_3	equilibrium constant of *trans*-2-butene and iso-butene
$C_{4,n}$	the concentration of 1-butene, mol kg^{-1}
$C_{4,c}$	the concentration of *cis*-2-butene, mol kg^{-1}
$C_{4,t}$	the concentration of *trans*-2-butene, mol kg^{-1}
$C_{4,i}$	the concentration of isobutene, mol kg^{-1}
C_4	the concentration of lumped butene, mol kg^{-1}
f(AO,$w$cor)	the correction function of main reactions
w	the weight fraction of sulfuric acid, wt %
$w$cor	the calibrated weight fraction of sulfuric acid

ABBREVIATIONS

C_5	*iso*-paraffins with carbon number 5
C_6	*iso*-paraffins with carbon number 6
C_7	*iso*-paraffins with carbon number 7
C_8	*iso*-paraffins with carbon number 8
DMH	dimethylhexane
TMP	trimethylpentane
C_9	*iso*-paraffins with carbon number 9
C_{10}	*iso*-paraffins with carbon number 10
C_{11}	*iso*-paraffins with carbon number 11
C_{12}	*iso*-paraffins with carbon number 12
HES	heavy hydrocarbon components
LES	light hydrocarbon components
AO	the volume ratio of acid to hydrocarbon
RON	research octane number

REFERENCES

(1) Hommeltoft, S. I. Isobutane alkylation - Recent developments, and future perspectives. *Appl. Catal., A* **2001**, *221*, 421−428.
(2) Akhmadova, K. K.; Magomadova, M. K.; Syrkin, A. M.; Yegutkin, N. L. History, current state and development prospects of process of isobutane alkylation with olefins. *Khim. Tekhnol.* **2018**, *19*, 101−118.
(3) Mou, J. N.; Qi, J.; Wang, Z.; Li, X. L.; Zhang, N. *Analysis on the Revisions of GB 17930-2016 "Gasoline for Motor Vehicles" Standard*, Standard Science, 2017; Vol. 3, pp 81−84.
(4) Busca, G. Acid catalysts in industrial hydrocarbon chemistry. *Chem. Rev.* **2007**, *107*, 5366−5410.
(5) Li, L.; Zhang, J.; Wang, K.; Luo, G. Caprolactam as a New Additive To Enhance Alkylation of Isobutane and Butene in H2SO4. *Ind. Eng. Chem. Res.* **2016**, *55*, 12818−12824.
(6) Weitkamp, J.; Traa, Y. Isobutane/butene alkylation on solid catalysts. Where do we stand? *Catal. Today* **1999**, *49*, 193−199.
(7) Querini, C. A. Isobutane/butene alkylation: regeneration of solid acid catalysts. *Catal. Today* **2000**, *62*, 135−143.
(8) Yoo, K.; Namboodiri, V. V.; Varma, R. S.; Smirniotis, P. G. Ionic liquid-catalyzed alkylation of isobutane with 2-butene. *J. Catal.* **2004**, *222*, 511−519.
(9) Feller, A.; Zuazo, I.; Guzman, A.; Barth, J. O.; Lercher, J. A. Common mechanistic aspects of liquid and solid acid catalyzed alkylation of isobutane with n-butene. *J. Catal.* **2003**, *216*, 313−323.
(10) Albright, L. F.; Li, K. W. Alkylation of Isobutane with Light Olefins Using Sulfuric Acid. Reaction Mechanism and Comparison with HF Alkylation. *Ind. Eng. Chem. Process Des. Dev.* **1970**, *9*, 447−454.
(11) Albright, L. F.; Spalding, M. A.; Faunce, J.; Eckert, R. E. Alkylation of isobutane with C4 olefins. 3. Two-step process using sulfuric acid as catalyst. *Ind. Eng. Chem. Res.* **1988**, *27*, 391−397.
(12) Martinis, J. M.; Froment, G. F. Alkylation on solid acids. Part 1. Experimental investigation of catalyst deactivation. *Ind. Eng. Chem. Res.* **2006**, *45*, 940−953.
(13) Ivashkina, E.; Dolganova, I.; Dolganov, I.; Ivanchina, E.; Nurmakanova, A.; Bekker, A. Modeling the H2SO4-catalyzed isobutane alkylation with alkenes considering the process unsteadiness. *Catal. Today* **2019**, *329*, 206−213.
(14) Schmerling, L. The Mechanism of the Alkylation of Paraffins. *J. Am. Chem. Soc.* **1945**, *67*, 1778−1783.
(15) Schmerling, L. The Mechanism of the Alkylation of Paraffins. II. Alkylation of Isobutane with Propene, 1-Butene and 2-Butene. *J. Am. Chem. Soc.* **1946**, *68*, 275−281.
(16) Li, K. W.; Eckert, R. E.; Albright, L. F. Alkylation of Isobutane with Light Olefins Using Sulfuric Acid. Operating Variables Affecting Physical Phenomena Only. *Ind. Eng. Chem. Process Des. Dev.* **1970**, *9*, 434−440.
(17) Mosby, J. F.; Albright, L. F. Alkylation of Isobutane with 1-Butene Using Sulfuric Acid as Catalyst at High Rates of Agitation. *Ind. Eng. Chem. Process Des. Dev.* **1966**, *5*, 183−190.
(18) Lee, L.-m.; Harriott, P. The Kinetics of Isobutane Alkylation in Sulfuric Acid. *Ind. Eng. Chem. Process Des. Dev.* **1977**, *16*, 282−287.
(19) Langley, J. R.; Pike, R. W. The kinetics of alkylation of isobutane with propylene. *AIChE J.* **1972**, *18*, 698−705.
(20) Schilder, L.; Maass, S.; Jess, A. Effective and Intrinsic Kinetics of Liquid-Phase Isobutane/2-Butene Alkylation Catalyzed by Chloroaluminate Ionic Liquids. *Ind. Eng. Chem. Res.* **2013**, *52*, 1877−1885.
(21) Sun, W.; Shi, Y.; Chen, J.; Xi, Z.; Zhao, L. Alkylation Kinetics of Isobutane by C4 Olefins Using Sulfuric Acid as Catalyst. *Ind. Eng. Chem. Res.* **2013**, *52*, 15262−15269.
(22) Kranz, K. Cold Temperature Alkylation Process. U.S. Patent 5,095,168 A, 1992.
(23) Meyers, R. A. *Handbook of Petroleum Refining Processes*; McGraw-Hill, 2003.
(24) Rodríguez, M. A.; Ancheyta, J. Detailed description of kinetic and reactor modeling for naphtha catalytic reforming. *Fuel* **2011**, *90*, 3492−3508.
(25) Cao, P.; Zheng, L.; Sun, W.; Zhao, L. Multiscale Modeling of Isobutane Alkylation with Mixed C4 Olefins Using Sulfuric Acid as Catalyst. *Ind. Eng. Chem. Res.* **2019**, *58*, 6340−6349.

https://doi.org/10.1021/acsomega.1c06850
ACS Omega 2022, 7, 9513−9526

(26) Wang, P.; Wang, D.; Xu, C.; Gao, J. DFT calculations of the alkylation reaction mechanisms of isobutane and 2-butene catalyzed by Brönsted acids. *Appl. Catal., A* **2007**, *332*, 22−26.
(27) Hofmann, J. E.; Schriesheim, A. Ionic Reactions Occurring During Sulfuric Acid Catalyzed Alkylation. II. Alkylation of Isobutane with C14-Labeled Butenes. *J. Am. Chem. Soc.* **1962**, *84*, 957−961.
(28) Doshi, B.; Albright, L. F. Degradation and Isomerization Reactions Occurring during Alkylation of Isobutane with Light Olefins. *Ind. Eng. Chem. Process Des. Dev.* **1976**, *15*, 53−60.
(29) Albright, L. F. Mechanism for Alkylation of Isobutane with Light Olefins. *Industrial and Laboratory Alkylations*; ACS Symposium Series; ACS, 1977; pp 128−146.
(30) Cai, H. b.; Dai, G. C. CFD Simulation of Fluid Flow in Sulfuric Acid Alkylation Reactor—Effect of Structure Parameters. *Huaxue Fanying Gongcheng Yu Gongyi* **2012**, *28*, 391−397.
(31) Cerqueira, H. S.; Caeiro, G.; Costa, L.; Ribeiro, F. R. Deactivation of FCC catalysts. *J. Mol. Catal. A: Chem.* **2008**, *292*, 1−13.
(32) Ellis, P. F. E.; Srinivasan, S.; Yap, K.-M. Prediction and Assessment of Corrosion in Sulfuric Acid Alkylation Units. In *Corrosion Conference and Expo 2013*: Orlando (US), 2013; pp 4797−4815.
(33) Berenblyum, A. S.; Katsman, E. A.; Berenblyum, R. A.; Hommeltoft, S. I. Modeling of side reactions of isobutane alkylation with butenes catalyzed trifluoromethane sulfonic acid. *Appl. Catal., A* **2005**, *284*, 207−214.
(34) Bartholomew, C. H. Mechanisms of catalyst deactivation. *Appl. Catal., A* **2001**, *212*, 17−60.
(35) Berenblyum, A. S.; Ovsyannikova, L. V.; Katsman, E. A.; Zavilla, J.; Hommeltoft, S. I.; Karasev, Y. Z. Acid soluble oil, by-product formed in isobutane alkylation with alkene in the presence of trifluoro methane sulfonic acid. *Appl. Catal., A* **2002**, *232*, 51−58.
(36) Dolganova, I. O.; Buryhina, E. S.; Ivashkina, E. N.; Bekker, A. V. Simulation of the high-octane alkylates manufacturing considering the process unsteadiness. *Pet. Sci. Technol.* **2018**, *36*, 514−519.
(37) Dormand, J. R. Methods for Stiff systems. In *Numerical Methods for Differential Equations*; CRC Press, 2018; pp 189−209.
(38) Lane, T. P.; Dumouchel, W. H. Simultaneous Confidence Intervals in Multiple Regression. *Am. Statistician* **1994**, *48*, 315−321.
(39) Zheng, W.; Li, D.; Sun, W.; Zhao, L. Multi-scale modeling of isobutane alkylation with 2-butene using composite ionic liquids as catalyst. *Chem. Eng. Sci.* **2018**, *186*, 209−218.

https://doi.org/10.1021/acsomega.1c06850
ACS Omega 2022, 7, 9513−9526